Investigation of Bulk Solid Material Load Profiles on a Belt Conveyor Test Rig

D. Ilic, T. Donohue, and C.A. Wheeler, Australia

This paper presents an investigation of active and passive stress states induced in bulk solid materials due to the transverse opening and closing of the conveyor belt. The relationship between active and passive stress states to the subsequent load profile exerted by the bulk solid material on the belt was modeled and examined using Discrete Element Modeling (DEM) simulations and results are compared to experimental results and existing theory

Key Words: *belt conveyor, load profile, discrete element modeling*

1 Introduction

As bulk solid material is transported between successive idler sets along a belt conveyor, active and passive stress states are induced in the bulk solid due to the constant opening and closing of the belt. When the belt is supported by an idler set, the belt and bulk solid are forced to conform to the troughing profile resulting in transverse compressive stresses.

Upon leaving the idler, the trough opens (due to gravity) allowing the bulk solid to relax transversely forming an active stress state. Upon reaching half to two thirds of the idler spacing the stress states theoretically reverse. A passive stress state is induced in the transverse direction resulting from compressive stresses due to the narrowing of the belt. The corresponding reaction loads on the belt influence the motion resistance of the belt conveyor [1].

Fig. 1: The test rig used for the experimental analysis.

Theoretical and experimental analysis of transverse bulk solid behaviour and the influence of bulk solid material properties on this motion has previously been undertaken in [1, 2] and [3, 4, 5] respectively. The work in this paper acts to further analyse and validate these interactions utilising DEM simulations.

Due to bulk solid material being transversely supported along the length of the conveyor by inclined sides of the belt, the approach in examining bulk solid motion on conveyor belts has been that the aforementioned process of active and passive stress states is analogous to the application of soil mechanics with respect to retaining wall structures. Pioneering research work in this area was undertaken by Krause and Hettler [6].

2 Active and Passive Stress States

Krause and Hettler [6] applied Coulomb's earth pressure theory to calculate the normal forces acting on the idler rolls of a belt conveyor. Based on this theory, for the active stress state, the slip plane angle θ_a to the horizontal as a function of the idler inclination angle β, bulk solid internal friction angle ϕ_i, belt and bulk solid friction angle ϕ_w and conveyor surcharge angle λ, can be given by:

$$\theta_a = \tan^{-1}\left(\frac{\left(\frac{\sqrt{\lambda_a \cdot \sin(\beta - \phi_w)}}{\sin(\beta + \lambda)}\right) \cdot \sin\lambda - \sin\phi_i}{\left(\frac{\sqrt{\lambda_a \cdot \sin(\beta - \phi_w)}}{\sin(\beta + \lambda)}\right) \cdot \cos\lambda - \cos\phi_i}\right) \quad (1)$$

where:

$$\lambda_a = \left(\frac{\sin(\beta + \phi_i)}{\sqrt{\sin(\beta - \phi_w)} + \sqrt{\frac{\sin(\phi_w + \phi_i) \cdot \sin(\phi_i - \lambda)}{\sin(\beta + \lambda)}}}\right)^2$$

Similarly for the passive stress state, the slip plane angle θ_p to the horizontal can be given by:

$$\theta_p = \tan^{-1}\left(\frac{\left(\frac{\sqrt{\lambda_p \cdot \sin(\beta + \phi_w)}}{\sin(\beta + \lambda)}\right) \cdot \sin\lambda + \sin\phi_i}{\left(\frac{\sqrt{\lambda_p \cdot \sin(\beta + \phi_w)}}{\sin(\beta + \lambda)}\right) \cdot \cos\lambda - \cos\phi_i}\right) \quad (2)$$

where:

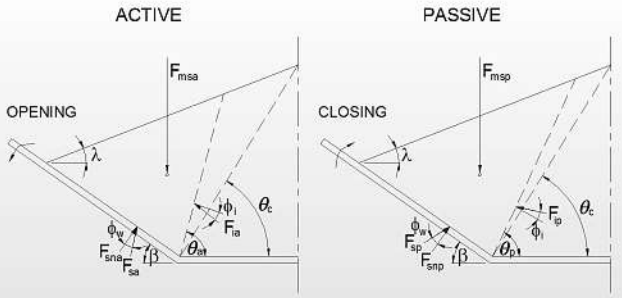

Fig. 2: Krause und Hettler's active and passive stress states.

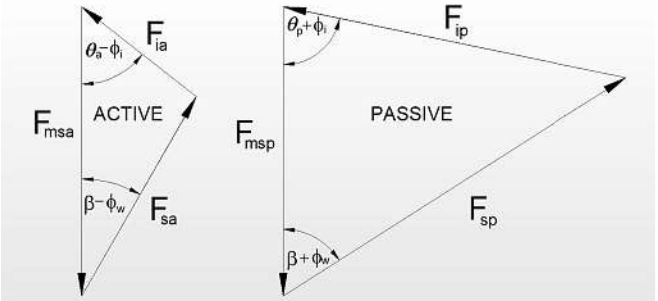

Fig. 3: Krause and Hettler's force vector diagrams for active and passive stress state.

$$\lambda_p = \left(\frac{\sin(\beta - \phi_i)}{\sqrt{\sin(\beta + \phi_w)} - \sqrt{\frac{\sin(\phi_w + \phi_i) \cdot \sin(\phi_i + \lambda)}{\sin(\beta + \lambda)}}} \right)^2$$

The active and passive slip plane angles θ_a and θ_p are illustrated in Fig. 2. Also shown in Fig. 2 is the angle from the idler junction to the centre of the top of bulk solid material pile θ_c.

The force vector diagrams showing equilibrium of forces acting in the active and passive stress states are shown in Fig. 3.

This paper investigates the forces associated with localized active and passive stress states for three bulk solid materials, river sand, gravel and magnetite. Investigations using experimental testing and DEM simulations were made and the results compared to those based on Krause and Hettler's theory.

3 Experimental Rig and Procedure

The test rig consists of a horizontal base section fixed to the ground, and two pivoting side sections (Fig. 1). The sides are attached to a frame (via turnbuckles) which is fixed to an oscillating plate and as the plate oscillates up and down the sides pivot. Two transparent walls are fixed at either end allowing for the observation of cross-sectional behaviour of the bulk solid as it is oscillated. A diagram of the rig is illustrated in Fig. 4.

The dimensions and configuration of the test facility were selected with the aim of comparing to an existing 600 mm wide re-circulating belt conveyor system with a three-roll idler troughing profile of 35° located at Tunra Bulk Solids laboratories.

The I-Scan matrix based pressure measurement system consists of a 55 × 55 mm (5051, 20 Psi) flexible tactile TekScan sensor, connected to the PC via an interface handle [4]. The position of the TekScan pad during testing is shown in Fig. 5. A number of tests were conducted with the pad located in the top position and bottom position as shown.

The bulk solid materials tested are shown in Fig. 6, and material properties and the active and passive slip plane angles based on Krause and Hettler's theory are shown in Table 1.

In general, the river sand particle size was in the range of 1 to 6 mm, gravel exhibited particles 5 to 30 mm and magnetite exhibited particles of 3 to 35 mm. Also, from observation, the magnetite material exhibited particles which were furthermost from spherical.

Each material was poured into the middle of the experimental rig and shaped manually in order to produce conveyor surcharge angles from Table 1 with the edge distance held constant at approximately 60 mm (as determined in [7]). The test rig was then oscillated at a frequency of 2.5 Hz and stroke of 12 mm for a period of 100 seconds during which data was recorded with the I-Scan software.

4 DEM Simulation and Calibration

The DEM simulations were performed using PFC3D v3.1 software [8], utilising a user defined contact model [9, 10] and modeling each material as spherical particles. All materials were calibrated and simulated as 5 mm particles only. Additionally, river sand was also calibrated and simulated as 2 to 5 mm particles, and magnetite and gravel materials were calibrated and simulated as 10 mm particles only.

Each simulated material was calibrated using angle of repose (AOR) tests and modifying correlated simulation parameters to suit based on experimental tests. The simulated angle of repose is shown in Table 2. The particle solids density was measured using a nitrogen displacement pycnometer and values are also shown in Table 2 as well as the number of particles for each simulation.

Table 1: Bulk solids material properties and slip plane angles.

Material	Wall friction angle ϕ_w [°]	Wall friction angle ϕ_i [°]	Angle of repose θ_R [°]	Conveyor surcharge angle λ [°]	Passive state slip angle θ_p [°]	Active state slip angle θ_a [°]
River sand	26	46	32-33	15	42	65
Gravel	32	45	32	13	38	56
Magnetite	30	57	37-38	23	40	70

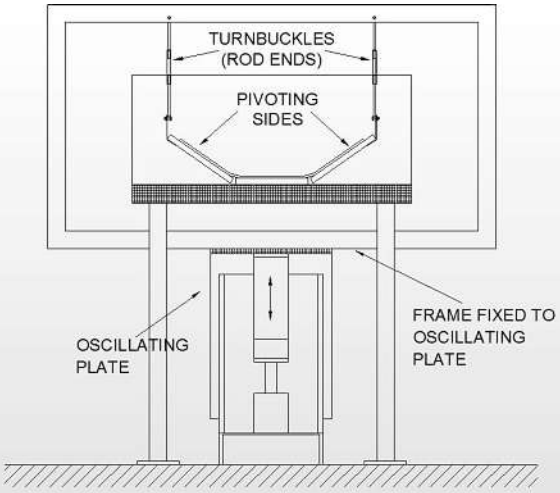

Fig. 4: Schematic drawing of the experimental test rig.

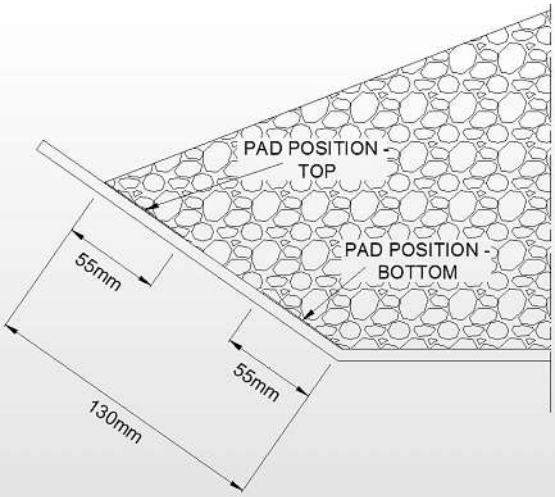

Fig. 5: Measuring positions of the TekScan pads.

The spherical particles were packed onto a cross section of the belt resembling that of the test rig (however only to a longitudinal length of 65 mm compared to 500 mm in experiments to minimize number of particles), with measurement 'zones' of 55 × 55 mm in top and bottom position on each side of simulated rig akin to that described in Fig. 5 and set to oscillate at the aforementioned constraints

5 Results and Discussion

Results from experimental testing and DEM simulations for river sand are shown in Fig. 7. Note that TekScan results are typical of entire 100 seconds of testing and are only shown for the first 50 seconds of the measurment perid for clarity between top and bottom pad. The results from experimental testing and DEM simulations for gravel and magnetite are shown in Figs. 8 and 9, respectively.

From the above results comparison, there is good overall correlation between the measured values obtained using TekScan and results obtained using DEM simulation analysis. The discrepancies are believed to be possibly due to the TekScan pad sensitivity range and also simulating each material as spherical particles only.

It is believed that materials consisting of non-spherical particles would show higher internal resistance to opening/closing due to the mechanical interlocking mechanisms representative of such materials. This was most evident for the magnetite material (top pad).

Also, for the DEM simulation, there was minimal influence of the particle size (within the range tested) on the overall values obtained. This presents the opportunity to investigate further

Table 2: Simulation properties.

Material	Simulated AOR [°]	Solids density [kg/m³]	Number of particles
River sand	32 - 34	2590	18.034 (5 mm) - 40.028 (2 - 5 mm)
Gravel	31 - 33	2582	17.506 (5 mm) - 2.082 (10 mm)
Magnetite	37 - 39	3665	20.676 (5 mm) - 2.471 (10 mm)

Table 3: Active and passive force and pressure based on Krause and Hettler's theory.

Material	Total active force [N/m]	Total normal active force [N]	Total normal active pressure [kPa]	Total passive force [N/m]	Total normal passive force [N]	Total normal passive pressure [kPa]
River sand	90	4.5	0.6	420.5	20.8	2.9
Gravel	116.9	5.5	0.8	453.8	21.2	3.0
Magnetite	139.9	6.7	0.9	1544.2	73.6	10.3

Note: F_{sa}: Total active force, F_{sp}: Total passive force
Pad length = 0.055 m, length of material on inclined side = 0.13 m
Total normal force =Total force × pad length × $\cos\theta_w$
Total normal pressure = Total normal force / (Pad length × length of material on inclined side)

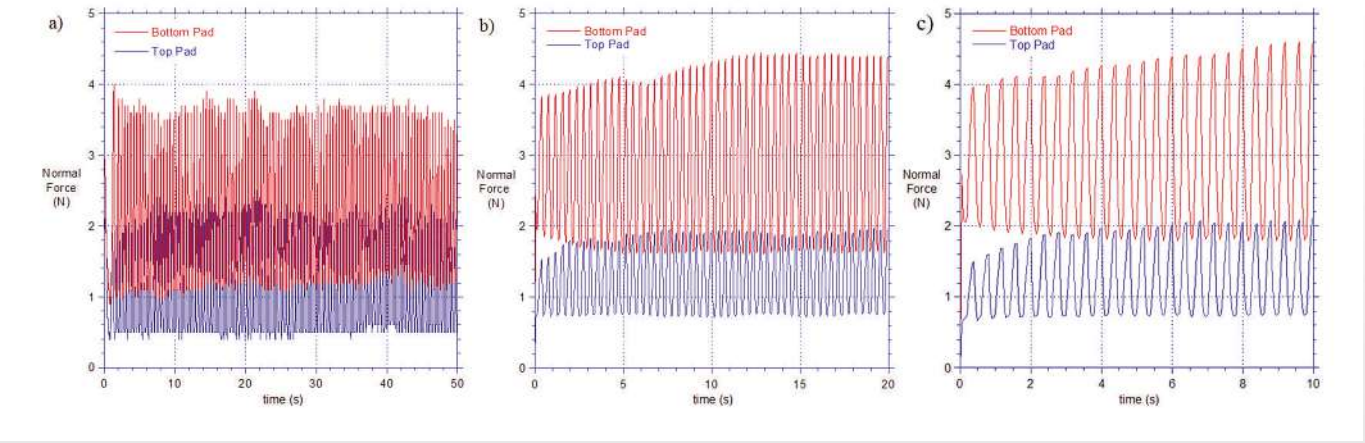

Fig. 7: Results from experimental testing and DEM simulations for river sand: a) TekScan results for 5 mm particles, b) DEM simulation results for 5 mm particles, c) DEM simulation results for 2 - 5 mm particles.

the minimum particle size necessary for DEM simulations in order to simulate real life bulk solid materials with valid results.

In addition to the experimental and DEM simulation forces comparison presented above, analysis was also conducted using DEM simulations to determine the load profile of the bulk solid material acting on the inclined sides of the belt (rig) and was compared to Krause and Hettler's theory. The results for each material are summarized in Figs. 10, 11 and 12.

For all simulated materials in the above figures, the normal pressure values when the belt (rig) was open were compared to the active and when the belt (rig) was closed were compared to the passive stress values as described in Section 2. Each resultant force was found by solving the force vector diagrams from Fig. 3, knowing the force due to the bulk solid material (under gravity) and the direction of the vectors.

The total active and passive normal pressure based on Krause and Hettler's theory was calculated for each material for the entire wedge and is presented in Table 3.

Referring to Figs. 10, 11 and 12 in view of results shown in Table 3, for the active stress state, there is good overall correlation between the measured values obtained using DEM simulation analysis and Krause and Hettler's theory. Figs. 10, 11 and 12 show that the maximum normal pressure when the belt is open is in the range of 0.5 to 1.2 kPa.

This is in good correlation with Krause and Hettler's theory which approximates the total normal active pressure to be in the range of 0.6 to 0.9 kPa. The figures also indicate that the maximum active stress occurs towards the idler junction and the minimum active stress occurs at the edge of the free top surface of material on inclined side.

For the passive stress state, results indicate that the measured values obtained from DEM simulations are lower than the theoretical values given by Krause and Hettler's theory, which leads to the postulation that perhaps the passive stress state is not fully developed within the cross section of the bulk solid material.

Interestingly, Figs. 10, 11 and 12 show that maximum normal pressure (on the inclined side) when the belt is closed occurs at a distance of 0.04 to 0.06 metres from the idler junction and not at the idler junction. That is, maximum stress (belt closing) occurs within 30 to 45 per cent of the length of the bulk solid material in contact with the inclined side (belt).

6 Conclusion

Results from the investigation indicate that there is good overall correlation between results from DEM simulations and the TekScan measurements for both the active (opening) and passive (closing) stress states.

Analysis from DEM simulations shows good correlation with Krause and Hettler's theory for the active stress state. This tends to indicate that the active stress state is fully developed within the material cross section due to the opening of the belt (rig).

Fig. 6: Samples of the tested materials.

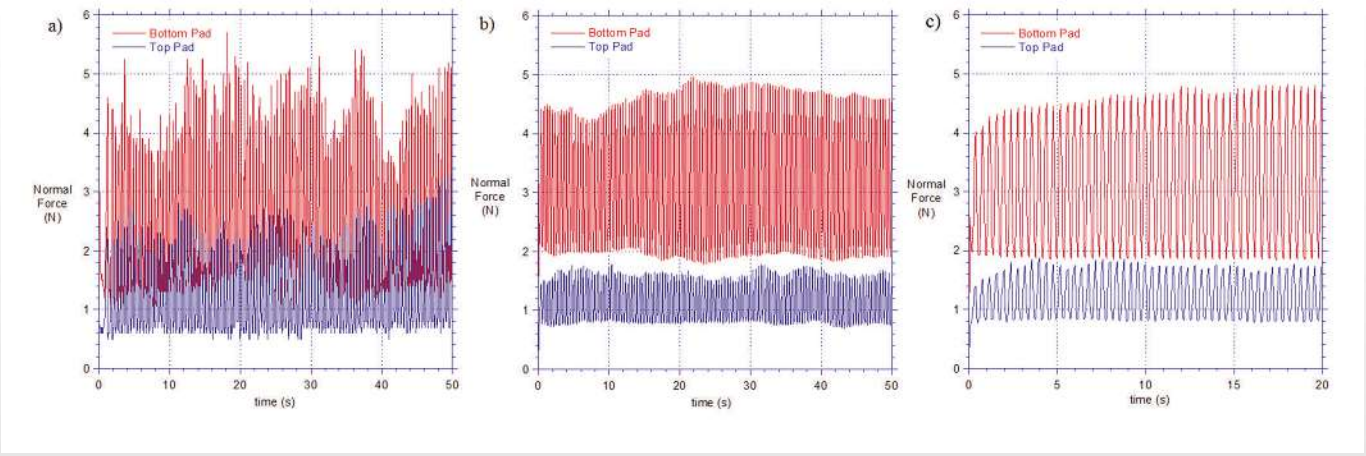

Fig. 8: Results from experimental testing and DEM simulations for gravel: a) TekScan results for 10 mm particles, b) DEM simulation results for 10 mm particles, c) DEM simulation results for 5 mm particles.

However, for the passive stress state, the data obtained from the DEM simulations indicates lower (significantly lower for magnetite) values than those calculated using Krause and Hettler's theory.

The investigation of bulk solid and conveyor belt interactions up to date further leads to the affirmation that either the passive stress state is not fully developed within the bulk solid material during belt closing or there is other material (particle) behaviour (interaction) present within the bulk solid material cross section than can be described by Krause and Hettler's theory.

References

[1] Wheeler, C.A.: *Analysis of the main resistances of belt conveyors*. PhD Thesis, The University of Newcastle, Australia, 2003.

[2] Roberts, A.W.: *Bulk solid and conveyor belt interactions for efficient transportation without spillage*. bulk solids handling, Vol. 18 (1996) No. 1, pp. 49-57.

[3] Ilic, D., Wheeler, C.A., and Roberts, A.W.: *Experimental investigation of bulk solid and conveyor belt interactions, conference proceedings*. 9th International Conference on Bulk Materials Storage, Handling and Transportation, University of Newcastle, NSW, Australia, 9-11th October, 2007.

[4] Ilic, D., Wheeler, C.A., and Roberts, A.W.: *An investigation of bulk solid stress states on a belt conveyor test rig*. Aggregates International, 06, 2008, pp. 6-13.

[5] Ilic, D., Donohue, T., and Wheeler, C.A.: *Discrete element modeling of bulk solid active and passive stress states on a belt conveyor test rig*. Conference Proceedings, CHoPS 2009 + ICBMH 2009, Brisbane, Australia, 3-7th August, 2009.

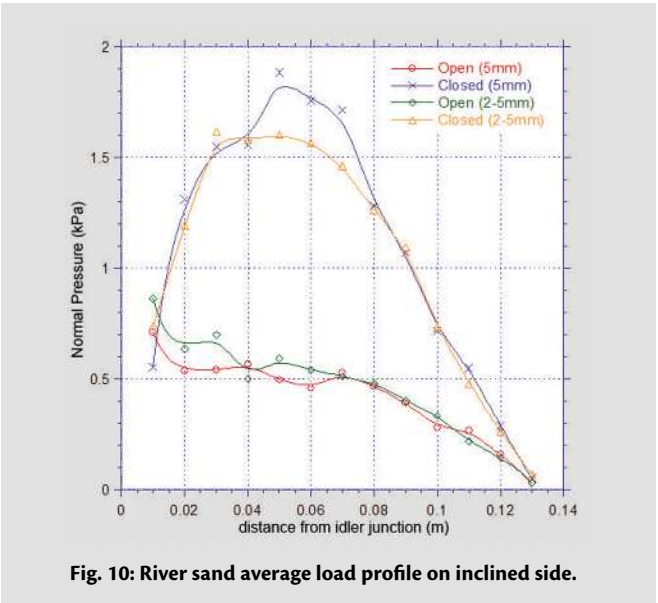

Fig. 10: River sand average load profile on inclined side.

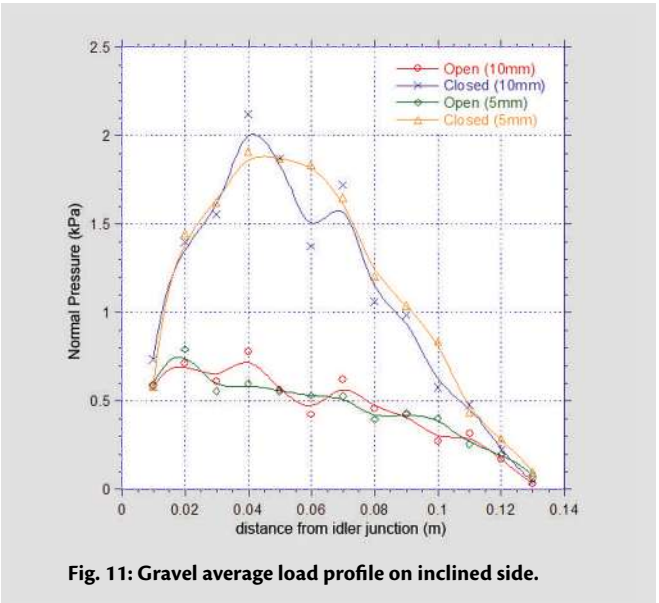

Fig. 11: Gravel average load profile on inclined side.

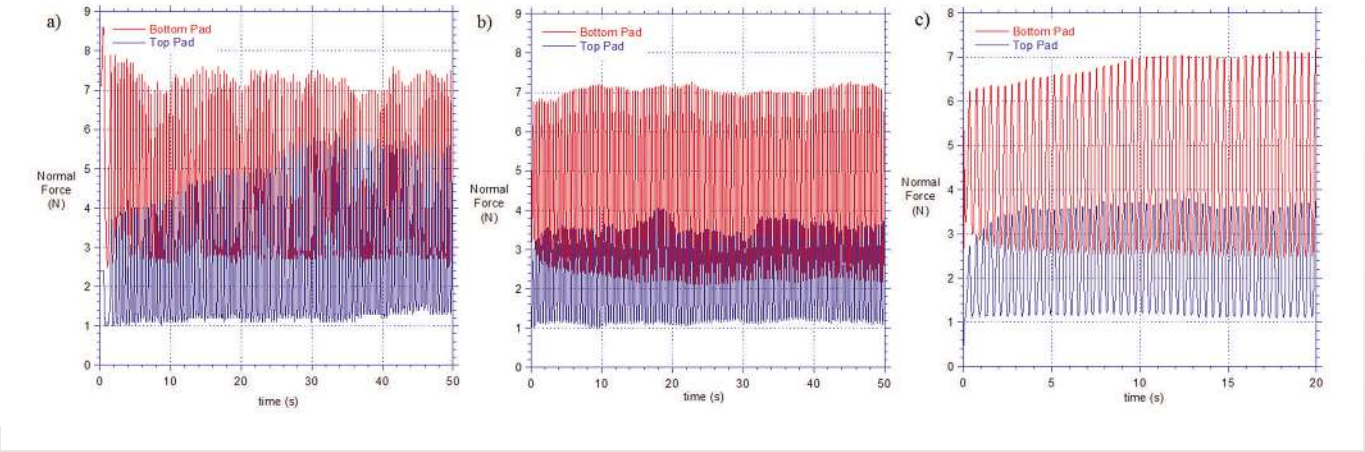

Fig. 9: Results from experimental testing and DEM simulations for magnetite: a) TekScan results for 10 mm particles, b) DEM simulation results for 10 mm particles, c) DEM simulation results for 5 mm particles.

[6] Krause, F. and Hettler, W.: Die *Belastung der Tragrollen von Gurtbandförderern mit dreiteiligen Tragrollenstationen infolge Fördergut unter Beachtung des Fördervorganges und der Schüttguteigenschaften*. Wissenschaftliche Zeitschrift der Technischen Hochschule Otto von Guericke, Magdeburg, 1974, 18, Heft 6/7, pp. 667-674.

[7] CEMA: *Belt conveyors for bulk materials*. 6th Edition, Conveyor Equipment Manufacturers Association (CEMA), USA, 2005.

[8] Itasca: *Particle flow code in three dimensions*. PFC3D v3.1 Manual, Itasca Consulting Group Minneapolis.

[9] Gröger, T. and Katterfeld, A.: *Application of the discrete element method in materials handling: basics and calibration*. bulk solid handling, Vol. 27 (2007) No. 1, pp. 17-23.

[10] Gröger, T., Tüzün, U. and Heyes, D.M.: *Modelling and measuring of cohesion in wet granular materials*. Powder Technology 133, 2003, pp. 203-215.

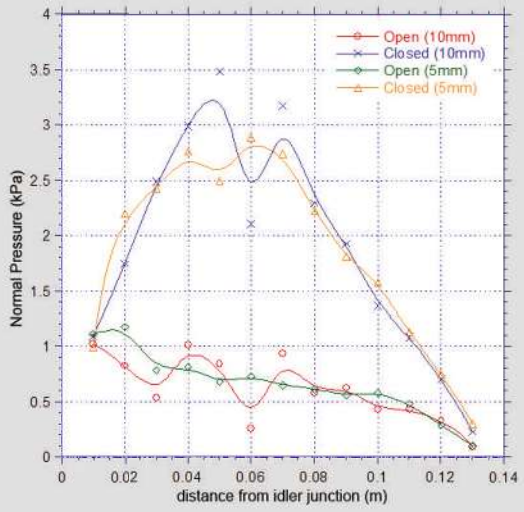

Fig. 12: Magnetite average load profile on inclined side.

About the Authors

Dusan Ilic (BE, MIEAust)

TUNRA Bulk Solids
The University of Newcastle
TA Building, University Drive,
Callaghan NSW 2308, Australia
Tel.: +61 2 4033 9010
Fax: +61 2 4033 9044
E-Mail: dusan.ilic@newcastle.edu.au

Dr. Timothy Donohue (BE, PhD)

TUNRA Bulk Solids
The University of Newcastle
TA Building, University Drive,
Callaghan NSW 2308, Australia
Tel.: +61 2 4033 9031
Fax: +61 2 4033 9044
E-Mail: timothy.donohue@newcastle.edu.au

Dr. Craig A. Wheeler (BE, MIEAust)

University of Newcastle
School of Engineering
University Drive,
Callaghan NSW 2308, Australia
Tel.: +61 2 4921 7018
Fax: +61 2 4921 6021
E-Mail: craig.wheeler@newcastle.edu.au